Mu Opioid Receptor (Oprm1) Copy Number Influences Nucleus Accumbens Microcircuitry and Reciprocal Social Behaviors

JNeurosci Accepted Manuscript

1 **Mu Opioid Receptor (Oprm1) Copy Number Influences Nucleus Accumbens Microcircuitry and**

2 **Reciprocal Social Behaviors**

3

4 **Abbreviated title**: Opioid deficit alters social circuits and behavior
5
6
7
8 Carlee Toddes[1], Emilia M. Lefevre[2], Dieter D. Brandner[1,3], Lauryn Zugschwert[4] & Patrick E. Rothwell[2,*]

9
10 [1]Graduate Program in Neuroscience, University of Minnesota, Minneapolis, MN, 55455

11 [2]Department of Neuroscience, University of Minnesota, Minneapolis, MN, 55455

12 [3]Medical Scientist Training Program, University of Minnesota, Minneapolis, MN, 55455

13 [4]Neuroscience Program & Department of Biology, University of St. Thomas, St. Paul, MN, 55105

14
15 *Corresponding Author:

16   Patrick E. Rothwell, Ph.D.
17   4-142 Wallin Medical Biosciences Building
18   2101 6th Street SE
19   Minneapolis, MN, 55455
20   Phone: 612-626-8744
21   Email: rothwell@umn.edu
22
23 Number of pages: 34
24 Number of figures: 7
25 Number of tables: 2
26
27 Number of words for abstract: 250 (out of 250 maximum)
28 Number of words for introduction: 648 (out of 650 maximum)
29 Number of words for discussion: 1,480 (out of 1,500 maximum)
30
31 **Conflict of interest statement**: The authors declare no competing financial interests.
32

ABSTRACT

The mu opioid receptor regulates reward derived from both drug use and natural experiences, including social interaction, through actions in the nucleus accumbens. Here, we studied nucleus accumbens microcircuitry and social behavior in male and female mice with heterozygous genetic knockout of the mu opioid receptor (Oprm1+/-). This genetic condition models the partial reduction of mu opioid receptor signaling reported in several neuropsychiatric disorders. We first analyzed inhibitory synapses in the nucleus accumbens, using methods that differentiate between medium spiny neurons (MSNs) expressing the D1 or D2 dopamine receptor. Inhibitory synaptic transmission was increased in D2-MSNs of male mutants, but not female mutants, while the expression of gephyrin mRNA and density of inhibitory synaptic puncta at the cell body of D2-MSNs was increased in mutants of both sexes. Some of these changes were more robust in Oprm1+/- mutants than Oprm1-/- mutants, demonstrating that partial reductions of mu opioid signaling can have large effects. At the behavioral level, social conditioned place preference and reciprocal social interaction were diminished in Oprm1+/- and Oprm1-/- mutants of both sexes. Interaction with Oprm1 mutants also altered the social behavior of wild-type test partners. We corroborated this latter result using a social preference task, in which wild-type mice preferred interactions with another typical mouse over Oprm1 mutants. Surprisingly, Oprm1-/- mice preferred interactions with other Oprm1-/- mutants, even though these interactions did not produce a conditioned place preference. Our results support a role for partial dysregulation of mu opioid signaling in social deficits associated with neuropsychiatric conditions.

SIGNIFICANCE STATEMENT

Activation of the mu opioid receptor plays a key role in the expression of normal social behaviors. In this study, we examined brain function and social behavior of female and male mice, with either partial or complete genetic deletion of mu opioid receptor expression. We observed abnormal social behavior following both genetic manipulations, as well as changes in the structure and function of synaptic input to a specific population of neurons in the nucleus accumbens, which is an important brain region for social behavior. Synaptic changes were most robust when mu opioid receptor expression was only partially lost, indicating that small reductions in mu opioid receptor signaling can have a large impact on brain function and behavior.

INTRODUCTION

Mu opioid receptor activation facilitates reward derived from social interaction and other natural experiences, as well as the abuse liability of exogenous opiate narcotics (Panksepp et al., 1980; Trezza et al., 2010; Darcq and Kieffer, 2018). Agonists with high mu opioid receptor affinity increase visual attention to faces in humans, and enhance social play behavior in juvenile rodents as well as marmosets, while pharmacological blockade of opioid receptors causes deficits in these behaviors (Guard et al., 2002; Chelnokova et al., 2016; Achterberg et al., 2019). Mu opioid receptor availability in the human nucleus accumbens is regulated by a variety of social circumstances (Hsu et al., 2013; Hsu et al., 2015), and intra-accumbal manipulations of mu opioid receptor activation can bidirectionally modulate social behavior in rodents (Trezza et al., 2011; Resendez et al., 2013; Smith et al., 2018). These findings are consistent with a general role for mu opioid receptor activation within the nucleus accumbens in motivated behavior (Baldo and Kelley, 2007; Richard et al., 2013; Castro and Bruchas, 2019).

Dysregulation of mu opioid receptor signaling may contribute to deficits in social interaction and other motivated behaviors that are a hallmark of neuropsychiatric disorders (Kennedy et al., 2006; Prossin et al., 2010; Pellissier et al., 2018; Ashok et al., 2019; Nummenmaa et al., 2020). Mice with constitutive genetic knockout of the mu opioid receptor (Oprm1) have behavioral deficits in social affiliation, attachment, and reward, as well as dramatic remodeling of synaptic architecture and gene expression in the nucleus accumbens (Moles et al., 2004; Cinque et al., 2012; Becker et al., 2014). These studies have focused on homozygous Oprm1-/- knockout mice, but the influence of Oprm1 haploinsufficiency on nucleus accumbens circuitry and social behavior has not been investigated. These are important unexplored issues, because partial loss of mu opioid receptor function (as modeled by the heterozygous Oprm1+/- genotype) is likely more relevant to functional deficits in human neuropsychiatric disorders.

To investigate these issues, we first evaluated the effects of mu opioid receptor copy number on nucleus accumbens circuitry, using female and male offspring of Oprm1+/- parents. This design allowed us to compare Oprm1+/- offspring with both Oprm1+/+ and Oprm1-/- littermates, permitting direct comparisons between all three genotypes while controlling for parental genotype. Analysis of synaptic gene expression, synaptic transmission, and synapse structure all revealed changes in Oprm1+/- mice, which in some cases

3

95   were greater than or equal to effects in Oprm1-/- mice. We also differentiated between effects on medium

96   spiny neurons that express dopamine receptor Drd1 (D1-MSNs) or Drd2 (D2-MSNs), since both dopamine

97   receptor subtypes contribute to social behavior but also have unique functions (Aragona et al., 2006; Gunaydin

98   et al., 2014; Manduca et al., 2016). These analyses provided novel information regarding sex differences in the

99   organization of nucleus accumbens inhibitory microcircuits, and revealed cell type-specific effects of Oprm1

100 copy number on D2-MSNs.

101   To determine whether these changes in nucleus accumbens microcircuits are accompanied by

102 alterations in social behavior, we tested Oprm1 mutant mice on a battery of social behavior assays. To

103 thoroughly evaluate all facets of reciprocal social interaction, we also quantified the social behavior of the

104 wildtype mice interacting with Oprm1 mutants during behavioral testing. Our results show impairments in social

105 behavior of Oprm1+/- as well as Oprm1-/- mice, which in turn change the behavior of wildtype mice in a

106 reciprocal fashion. Abnormal social behavior of Oprm1 mutant mice was also apparent in a real-time social

107 preference test (Shah et al., 2013), where wildtype mice chose to avoid social interaction with Oprm1-/- mice.

108 Conversely, Oprm1-/- mutant mice chose to engage in social interaction with other Oprm1-/- mutants, even

109 though this interaction did not produce a conditioned place preference (CPP). Our findings reveal fundamental

110 dissociations between different facets of social behavior, and demonstrate that partial reductions of mu opioid

111 signaling can have large effects on brain function and behavior, which may contribute to social deficits

112 associated with neuropsychiatric conditions.

113

114 **MATERIALS AND METHODS**

115

116 **Subjects**

117   Experiments were performed with female and male Oprm1 knockout mice (Matthes et al., 1996). For

118 electrophysiology and immunohistochemistry analyses, Oprm1 mutant mice were crossed with Drd1a-

119 tdTomato BAC transgenic mice (Shuen et al., 2008) and Drd2-eGFP BAC transgenic mice (Gong et al., 2003).

120 All genetically modified strains were maintained on a C57Bl/6J genetic background, and distinct groups of

121 wildtype C57Bl/6J mice with no Oprm1 mutant ancestry were used as novel stimulus mice for testing social

4

122   behavior. To avoid ambiguity, we refer to these mice as "C57Bl/6J", whereas we refer to wildtype mice

123   generated from Oprm1 breeding colonies as "Oprm1+/+". Mice were housed in groups of 2-5 per cage, on a 12

124   hour light cycle (0600h – 1800h) at ~23° C with food and water provided ad libitum. Experimental procedures

125   were conducted between 1000h – 1600h, and were approved by the Institutional Animal Care and Use

126   Committee of the University of Minnesota.

127

128   **Gene Expression**

129   Quantitative RT-PCR was performed on nucleus accumbens tissue punches containing the core and

130   shell subregions, as previously described (Lefevre et al., 2020). Tissue was snap frozen on dry ice and stored

131   at -80°C. RNA was isolated using the RNeasy Mini Kit (Qiagen) according to the manufacturer's instructions.

132   All RNA samples had A260/A280 purity ratio ≥ 2. Reverse transcription was performed using Superscript III

133   (Invitrogen). For each sample, duplicate cDNA preparations were set up. Mouse β-actin mRNA was used as

134   the endogenous control to measure differences in expression of Oprm1, Gphn, Slc32a1, Arhgef9, Dlg1, Dlg3,

135   and Dlg4. Primer sequences for measurement of each mRNA can be found in Table 1. Quantitative RT-PCR

136   using SYBR green (BioRad, Hercules, CA) was carried out with a Lightcycler 480 II (Roche) system with the

137   following cycle parameters: 1 x (30 sec @ 95°C), 35 x (5 sec @ 95°C followed by 30 sec @ 60°C). Data were

138   analyzed by comparing the C(t) values of the treatments tested using the ΔΔC(t) method. Expression values of

139   target genes were first normalized to the expression value of β-actin. The mean of cDNA replicate reactions

140   was used to quantify the relative target gene expression.

141

142   **Behavioral Responses to Morphine Administration**

143   Measurement of thermal antinociception and open field locomotion after morphine administration were

144   performed as previously described (Lefevre et al., 2020). We tested open-field locomotor activity in a clear

145   plexiglass arena (ENV-510, Med Associates) housed within a sound-attenuating chamber. The location of the

146   mouse within the arena was tracked in two dimensions by arrays of infrared beams, connected to a computer

147   running Activity Monitor software (Med Associates). Mice were habituated to the chamber for one hour the day

148   before initiating drug treatment. The next day, animals were tested in the open field chamber after injection of

149 saline (s.c.). They were then tested on the following doses of morphine (2.0, 6.32, 20 mg/kg), receiving an

150 incremental increase in dose every day. The session duration varied as a function of dose: 60 mins (saline and

151 2 mg/kg), 90 mins (6.32 mg/kg), or 120 mins (20 mg/kg). To facilitate comparison between sessions of different

152 length, distance travelled is presented in units of meters per hour (m/hr).

153   Thermal antinociception was tested on a 55°C hot plate (IITC Life Scientific). The day before initiating

154 drug treatment, mice were habituated to the instrument for 60 seconds at room temperature. We then

155 established baseline latency to either jump or lift and lick a hind paw at 55°C. Mice were then tested 30

156 minutes after injection of saline or morphine, with a maximal cutoff of 30 seconds to prevent tissue damage.

157 The percent maximum possible effect was calculated as (test latency – baseline latency) / (30 sec – baseline

158 latency) x 100.

159

160 **Electrophysiology**

161   Whole-cell voltage-clamp recordings from nucleus accumbens MSNs in acute brain slices were

162 performed as previously described (Pisansky et al., 2019). Parasagittal slices (240 µm) containing the nucleus

163 accumbens were prepared from Oprm1+/+, Oprm1+/-, and Oprm1-/- mice carrying the Drd1-tdTomato and/or

164 Drd2-eGFP reporter gene. These mice were offspring of Oprm1+/- heterozygous parents and had not

165 undergone any behavioral testing. Mice were anesthetized with isoflurane and decapitated, brains quickly

166 removed and placed in ice-cold cutting solution containing (in mM): 228 sucrose, 26 NaHCO3, 11 glucose, 2.5

167 KCl, 1 NaH2PO4-H2O, 7 MgSO4-7H20, 0.5 CaCl2-2H2O. Slices were cut by adhering the lateral surface of

168 the brain to the stage of a vibratome (Leica VT1000S), and allowed to recover for a minimum of 60 min in a

169 submerged holding chamber (~25°C) containing artificial cerebrospinal fluid (aCSF) containing (in mM): 119

170 NaCl, 26.2 NaHCO3, 2.5 KCl, 1 NaH2PO4-H2O, 11 glucose, 1.3 MgSO4-7H2O, 2.5 CaCl2-2H2O. Slices were

171 transferred to a submerged recording chamber and continuously perfused with aCSF at a rate of 2 mL/min at

172 room temperature. All solutions were continuously oxygenated (95% O_2/5% CO_2). To pharmacologically

173 isolate miniature inhibitory post-synaptic currents (mIPSCs), we added TTX (0.5 µM) to block spontaneous

174 activity and D-APV (50 mM) and NBQX (10 mM) to block NMDARs and AMPARs, respectively.

175   Whole-cell recordings from MSNs in the nucleus accumbens medial shell were obtained under visual

176   control using IR-DIC optics on an Olympus BX51W1 microscope. Red and green fluorescence were used to

177   identify D1-MSNs and D2-MSNs, respectively. Voltage-clamp recordings were made with borosilicate glass

178   electrodes (2–5 Mohm) filled with (in mM) 120 CsMeSO4, 15 CsCl, 10 TEA-Cl, 8 NaCl, 10 HEPES, 1 EGTA, 5

179   QX-314, 4 ATP-Mg, 0.3 GTP-Na (pH 7.2-7.3). MSNs were voltage clamped at 0 mV to increase the driving

180   force for current flow through $GABA_A$ receptors. Recordings were performed using a MultiClamp 700B amplifier

181   (Molecular Devices), filtered at 2 kHz, and digitized at 10 kHz. Data acquisition and analysis were performed

182   online using Axograph software. Series resistance was monitored continuously and experiments were

183   discarded if resistance changed by >20%. At least 200 events per cell were acquired in 15 s blocks and

184   detected using a threshold of 5 pA; all events included in the final data analysis were verified by eye.

185

186   **Immunohistochemistry and Confocal Microscopy**

187   Oprm1+/+, Oprm1+/-, and Oprm1-/- mice carrying the Drd2-eGFP reporter gene were deeply

188   anesthetized using sodium pentobarbitol (Fatal-Plus, Vortech Pharmaceuticals) and transcardially perfused

189   with ice cold 0.01 M PBS followed by ice cold 4% PFA in 0.01 M PBS.. Brains were removed and post-fixed 24

190   hours in 4% PFA in PBS. The following day, brains were rinsed briefly with 0.01 M PBS and sectioned in the

191   coronal plane at 50 um. Tissue sections were blocked for 1 hour in blocking buffer (2% NHS, 0.2% triton x 100,

192   and 0.05% Tween20 in 0.01 M PBS) and exposed to rabbit anti-GFP (1:1000, Abcam #ab290, to label D2-

193   MSN somata) and mouse anti-Gephyrin (1:250, Synaptic Systems #147077, to label inhibitory synapses),

194   diluted in blocking buffer. After 24 hours at 4° C, sections were rinsed in wash buffer (Tris-buffered saline with

195   0.1% Tween20) and exposed to anti-Rabbit A488 (1:1000, Abcam #ab150073) and anti-Mouse A647

196   secondary antibodies (1:1000, Abcam #ab150115) overnight at 4° C.

197   Stained tissue sections were imaged on a Leica TCS SPE laser scanning confocal microscope (Leica

198   Microsystems, Wetzlar, Germany). A minimum of 3 image stacks per hemisphere were collected from D2-

199   MSNs in the nucleus accumbens of each section, centered on the border between core and medial shell

200   (including both subregions). Image stacks were collected with a Leica 63X HCX PL APO objective with

201   numerical aperture of 1.4, using laser and PMT settings optimized for excitation and emission of Alexa A488

202 and A647. Digital zoom between 8x and 10x was applied and stacks were collected at 2048 by 2048 pixel

203 resolution using a step size of 0.3 µm and 1 airy unit pinhole diameter. Image stacks were imported into Imaris

204 9.0 (Bitplane, Zurich, Switzerland) and analyses were conducted on 3D renderings of compiled confocal

205 stacks. A surface object was applied to the A488 channel to produce a surface representing the GFP-

206 expressing somata in the image stack. Using this surface as a mask, the portion of the A647 channel

207 contained within this surface was isolated to restrict our analysis to individual D2-MSNs. The spot detection

208 algorithm (Banovic et al., 2010) was used to detect gephyrin puncta in the masked A647 channel. A second

209 algorithm was applied to restrict spots within 1 µm of the GFP immunoreactive surface object. Puncta area

210 density was calculated as the ratio of detected A647 spots to area of the surface object.

211

212 **Assays of Social Behavior**

213   To evaluate social behavior, we used a battery of previously described assays: social CPP (Panksepp

214 and Lahvis, 2007; Cinque et al., 2012; Dolen et al., 2013); the standard three-chamber test of sociability and

215 preference for social novelty (Nadler et al., 2004); reciprocal social interaction (Terranova and Laviola, 2005);

216 and a real-time preference test for social interaction (Shah et al., 2013). Animals were moved to an isolated

217 testing room 1 hour before tests of social behavior. All experiments were conducted at 60-70 luminosity, and at

218 temperature conditions equal to those of the animal housing facility. Experimental sessions were video

219 recorded and, for social CPP and the three-chamber test, behavioral data was analyzed using ANY-maze

220 behavioral tracking software. Dyadic social interaction was hand scored by researchers blind to experimental

221 conditions. With the exception of social CPP (described below), all tests of social behavior involved novel

222 social partners that were not siblings or cage mates.

223   Social CPP: mice were weaned at 3 weeks of age into home cages containing 3-5 littermates and

224 housed on corn-cob bedding. The social CPP procedure began one week after weaning, to permit comparison

225 with previous studies of Oprm1-/- mice (Cinque et al., 2012). The CPP test apparatus (18" x 10" x 8") was

226 divided into two equally sized zones by a clear plastic wall, with an oval opening (2" x 1.5") at the base. The

227 floor of each zone was covered with a different type of novel bedding (cellunest or small animal pellet bedding,

228 PetSmart), with the chamber cleaned and fresh bedding added for each mouse. The protocol began with a

8

229 baseline CPP session, with each mouse tested individually and allowed to freely explore the apparatus for 10

230 minutes. Behavior was video-recorded and time spent in each zone was analyzed automatically using ANY-

231 maze behavioral tracking software. After establishing baseline preference for the two different beddings, mice

232 were assigned to receive social conditioning with littermates from the same home cage for 24 hours on one

233 type of bedding, followed by 24 hours in social isolation on the other type of bedding. The assignment of each

234 bedding to social or isolation conditioning was counterbalanced for an unbiased design. After isolation

235 conditioning, animals were individually returned to the CPP apparatus for a 10 minute test session. A

236 "preference score" was calculate by taking difference between time spent in the social zone on test versus

237 baseline.

238   Three-chamber social test: mice were tested at 6-8 weeks of age, to permit comparison with previous

239 studies of Oprm1-/- mutants (Becker et al., 2014). The test apparatus was a white plastic rectangular box (25"

240 x 15"x 8") consisting of three interconnected chambers. Two identical wire cups were placed on each end of

241 the apparatus. Prior to testing, mice were habituated to the empty apparatus for 10 minutes of free exploration.

242 During the sociability test, an age- and sex-matched C57Bl/6J stimulus mouse was introduced in one wire cup,

243 whereas the other cup was left empty. The experimental mouse was then allowed to freely explore all three

244 chambers for ten minutes. The social memory portion of the test began immediately thereafter, with a novel

245 age- and sex-matched C57Bl/6J stimulus mouse introduced into the previously empty wire cup. The

246 experimental mouse was then allowed to freely explore all three chambers for ten minutes. All three phases

247 were recorded by a video camera, and time spent by the experimental mouse in each chamber and in

248 proximity of each cylinder (<2 cm) was measured by ANY-maze tracking software. After each test, the entire

249 apparatus was cleaned with 70% ethanol.

250   Reciprocal social interaction test: mice were tested at 6-8 weeks of age, to permit comparison with

251 previous studies of Oprm1-/- mutants (Becker et al., 2014). The test apparatus was an opaque white

252 rectangular box with 1 cm of fresh corn cob bedding on the floor. Experimental mice (Oprm1 mutants) were

253 introduced to an age- and sex-matched stimulus mouse in the testing apparatus for 10 min. Each stimulus

254 mouse was either a novel C57Bl/6J mouse, or a novel Oprm1 mutant from a different litter but with the same

255 genotype as the experimental mouse (Becker et al., 2014), and was only used as a stimulus mouse for a single

9

256   test session. Video recordings of various social behaviors exhibited by experimental and stimulus mice were

257   hand scored by a blinded experimenter using Button Box 5.0 (Behavioral Research Solutions, LLC). Social

258   behaviors were categorized into one of the following groups: nose-nose interaction (direct investigation of

259   orofacial region), huddling (stationary sitting next to partner), social exploration (anogenital investigation, social

260   sniffing outside of orofacial region, social grooming), and following (Terranova and Laviola, 2005). The sum of

261   these social behaviors were used for "Total Interaction Duration". A small number of videos were lost due to

262   technical errors before these specific behaviors could be scored, resulting in a smaller sample size in behavior

263   breakdowns compared to total interaction duration.

264   Real-time social preference test: this assay was based on a published protocol that allows a "judge" to

265   choose between interacting with a "typical" (Oprm1+/+) and an "atypical" (Oprm1 mutant) mouse (Shah et al.,

266   2013). To maintain consistency with other assays of social behavior, mice were tested at 6-8 weeks of age,

267   using the same three-chamber social testing apparatus described above. Judges were habituated for 10

268   minutes prior to testing in the empty apparatus. After habituation, two wire cups were placed in either end

269   chamber: one contained the Oprm1+/+ mouse, and the other contained either a Oprm1+/- or Oprm1-/- mutant.

270   Judges were then allowed to freely explore the chamber for 30 minutes. Test sessions were recorded by a

271   video camera and the time the target mouse spent in each chamber and in proximity of each cylinder (<2 cm)

272   was measured by ANY-maze tracking software. After each test, the entire apparatus was cleaned with 70%

273   ethanol.

274

275   **Experimental Design and Statistical Analyses**

276   Oprm1 mutant mice were generated using three different breeding schemes. The first breeding strategy

277   involved parents that were both Oprm1+/-, generating littermate offspring with a mix of all possible genotypes.

278   This strategy was used to generate mice for analysis of gene expression, behavioral responses to morphine,

279   electrophysiology, and immunohistochemistry. However, one drawback of this strategy is that Mendelian

280   inheritance from Oprm1+/- parents leads to a larger number of Oprm1+/- offspring (50%), relative to Oprm1-/-

281   (25%) or Oprm1+/+ (25%). For assessment of social behavior, we needed to obtain large and comparable

282   numbers of all three genotypes. We therefore analyzed social behavior using offspring from Oprm1+/- parents,

10

283 as well as age-matched offspring of parents that were both Oprm1+/+ (generating only Oprm1+/+ offspring) or

284 Oprm1-/- (generating only Oprm1-/- offspring). For social behavior experiments, this means Oprm1+/+ mice

285 were raised by parents that were either Oprm1+/+ or Oprm1+/-, and Oprm1-/- mice were raised by parents that

286 were either Oprm1+/- or Oprm1-/-. For each assay of social behavior, we report values obtained from mice of

287 the same genotype generated by different breeding strategies, and pool data from different breeding strategies

288 when results are comparable.

289 Similar numbers of male and female animals were used in all experiments, with samples size indicated

290 in figure legends. Individual data points from males (filled circles) and females (open circles) are distinguished

291 in figures. Sex was included as a variable in factorial ANOVA models analyzed using IBM SPSS Statistics v24,

292 with repeated measures on within-subject factors. Main effects of sex and interactions involving sex were not

293 significant unless noted otherwise. For main effects or interactions involving repeated measures, the Huynh-

294 Feldt correction was applied to control for potential violations of the sphericity assumption. This correction

295 reduces the degrees of freedom, resulting in non-integer values. Significant interactions are indicated in figures

296 by a red asterisk, and were decomposed by analyzing simple effects (i.e., the effect of one variable at each

297 level of the other variable). Significant main effects were analyzed using LSD post-hoc tests, denoted by black

298 asterisks above the data. Effect sizes are expressed as partial eta-squared (η_p^2) values. The Type I error rate

299 was set to $\alpha=0.05$ (two-tailed) for all comparisons. All summary data are displayed as mean $\pm$ SEM.

300

301 **RESULTS**

302 **Functional Validation of Partial Genetic Knockout in Oprm1+/- Mutant Mice**

303 To compare Oprm1+/- and Oprm1-/- mice with Oprm1+/+ littermates, we first studied female and male

304 offspring generated by breeding two Oprm1+/- parents (Figure 1A). We used quantitative RT-PCR to measure

305 Oprm1 expression in nucleus accumbens tissue punches from all three genotypes (Figure 1B). There was a

306 complete loss Oprm1 expression in the nucleus accumbens of Oprm1-/- mice, with a partial (~35%) reduction

307 of expression in Oprm1+/- mice ($F_{2,32}=64.19$, $p<0.001$, $\eta_p^2=0.80$). To confirm that this reduction in Oprm1

308 expression has functional consequences, we injected mice of all three genotypes with ascending doses of

309 morphine, and measured open field activity as well as thermal nociception on a hot plate. In the open field

11

310   (Figure 1C), Oprm1-/- mice did not exhibit dose-dependent increases in hyperlocomotion, while the behavioral

311   response of Oprm1+/- mice was attenuated but not completely absent (Genotype x Dose interaction:

312    $F_{4.33,58.50}$=48.30, p<0.001, η_p^2=0.78). On the hot plate (Figure 1D), dose-dependent changes in thermal

313   antinociception were attenuated in both Oprm1-/- and Oprm1+/- mice to a similar extent (Genotype x Dose

314   interaction: $F_{6,78}$=7.38, p<0.001, η_p^2=0.36). These findings are consistent with previous publications (Matthes et

315   al., 1996; Sora et al., 2001), and support the notion that both Oprm1 alleles contribute to expression of

316   functional receptors (Kieffer and Gaveriaux-Ruff, 2002).

317

318   **Oprm1 Copy Number Affects Synaptic Gene Expression in the Nucleus Accumbens**

319   Oprm1-/- mice have substantially more symmetrical synapses in the nucleus accumbens, with

320   increased expression of many inhibitory synaptic genes (Becker et al., 2014). We used nucleus accumbens

321   tissue samples to measure mRNA expression of several inhibitory synaptic molecules in all three genotypes

322   (Figure 2A). The expression of gephyrin (Figure 2B), an inhibitory postsynaptic scaffolding protein (Tyagarajan

323   and Fritschy, 2014), was significantly increased in both Oprm1-/- and Oprm1+/- mutants compared to

324   Oprm1+/+ controls ($F_{2,23}$=3.81, p=0.037, η_p^2=0.25). The expression of VGAT (Figure 2C), the vesicular GABA

325   transporter, was significantly increased in Oprm1-/- mutants ($F_{2,23}$=4.06, p=0.031, η_p^2=0.26). Genotype did not

326   affect expression of collybistin (Figure 2D), a GDP-GTP exchange factor that facilitates gephyrin trafficking

327   (Kins et al., 2000). However, there was a main effect of Sex for expression of both VGAT ($F_{1,23}$=10.33,

328   p=0.004, η_p^2=0.31) and collybistin ($F_{1,23}$=23.47, p<0.001, η_p^2=0.50), with higher expression of both genes in

329   male mice. We also measured mRNA expression of PSD-95 (Dlg4) and other excitatory synaptic scaffolding

330   molecules in the membrane-associated guanylate kinase family (Won et al., 2017). Oprm1 mutants did not

331   have detectable differences in expression of Dlg1 (Figure 2E), Dlg3 (Figure 2F), or Dlg4 (Figure 2G). Previous

332   studies found no changes in the number of asymmetrical synapses in the nucleus accumbens of Oprm1-/-

333   mice (Becker et al., 2014), suggesting a stronger influence of Oprm1 copy number on inhibitory synapses in

334   the nucleus accumbens.

335

336   **Oprm1 Copy Number Affects the Function and Structure of Nucleus Accumbens Inhibitory Synapses**

12

337   Given the increased expression of inhibitory synaptic genes in Oprm1 mutant mice, we next assessed

338   functional changes in synaptic transmission within the nucleus accumbens. To selectively analyze changes in

339   D1- and D2-MSNs, we crossed Oprm1 knockout mice with double-transgenic fluorescent reporter mice

340   expressing Drd1-tdTomato and Drd2-eGFP. In acute brain slices prepared from these animals, we performed

341   whole-cell voltage-clamp recordings from red D1-MSNs and green D2-MSNs (Figure 3A-B), and measured the

342   frequency and amplitude of miniature inhibitory postsynaptic currents (mIPSCs). In Oprm1+/+ control mice,

343   there was a noteworthy sex difference in basal synaptic transmission (Cell Type x Sex interaction: $F_{1,30}$=7.19,

344   p=0.012, η_p^2=0.19), with larger mIPSC amplitude in male D1-MSNs and female D2-MSNs.

345   For mIPSC amplitude (Figure 3C-F), omnibus ANOVA revealed a significant Cell Type x Sex x

346   Genotype interaction ($F_{2,113}$=3.31, p=0.040, η_p^2=0.06). There were no significant effects on mIPSC amplitude in

347   D1-MSNs (Figure 3C), but for D2-MSNs (Figure 3E), there was a significant Sex x Genotype interaction

348   ($F_{2,61}$=3.62, p=0.033, η_p^2=0.11). This interaction was driven by a main effect of Genotype in male mice

349   ($F_{2,39}$=4.52, p=0.017, η_p^2=0.19), but not in female mice. In D2-MSNs from male mice, mIPSC amplitude was

350   significantly higher in Oprm1+/- and Oprm1-/- mutants relative to Oprm1+/+ controls. For mIPSC frequency

351   (Figure 3G-J), there were no significant main effects or interactions in an omnibus ANOVA. However, we noted

352   a trend toward a main effect of Genotype in D2-MSNs from male mice ($F_{2,39}$=3.18, p=0.053, η_p^2=0.14), with

353   higher mIPSC frequency in Oprm1+/- mutants relative to Oprm1+/+ controls.

354   Inhibitory synapses formed at different subcellular locations generate quantal currents with distinct

355   biophysical properties (Koos et al., 2004; Straub et al., 2016). Perisomatic inhibitory synapses generate

356   currents with larger amplitude, while inhibitory synapses in the dendritic arbor generate currents with smaller

357   amplitude (Figure 4A). When we analyzed mIPSC frequency from male D2-MSNs as a function of amplitude

358   (Figure 4B), we found Oprm1+/- and Oprm1-/- males had a specific increase in the frequency of currents with

359   amplitude larger than 10 pA (Genotype x Amplitude interaction: $F_{2,39}$=6.13, p=0.005, η_p^2=0.24), suggesting

360   Oprm1 copy number affects perisomatic inhibitory synapses. To visualize these synapses, we performed

361   immunohistochemistry for gephyrin in D2-eGFP reporter mice (Gittis et al., 2011), so green fluorescence could

362   be used to construct a soma mask and quantify perisomatic gephyrin puncta (Figure 4C-D). The mean density

363   of perisomatic gephyrin puncta was doubled in Oprm1+/- mutants (Figure 4E), with a significant but less

364 dramatic increase Oprm1-/- mutants ($F_{2,11}$=24.55, p<0.001, η_p^2=0.82). Unlike the functional changes in synaptic

365 transmission (Figure 3), these structural synaptic changes did not appear to differ between sexes, which is

366 consistent with the elevated expression of gephyrin mRNA in nucleus accumbens tissue from both sexes

367 (Figure 2). Together, our results indicate that Oprm1 copy number alters both form and function of inhibitory

368 microcircuits in the nucleus accumbens.

369

370 **Oprm1 Copy Number Alters Social Reward**

371 Perisomatic inhibitory synapses onto MSNs tend to originate from fast-spiking interneurons (Gittis et al.,

372 2011; Straub et al., 2016). In the nucleus accumbens, fast-spiking interneurons regulate the development of

373 CPP (Wang et al., 2018; Chen et al., 2019), and previous reports indicate Oprm1-/- mutants fail to develop

374 social CPP (Cinque et al., 2012). To extend this analysis to Oprm1+/- mice, we used a social CPP protocol that

375 began with 24 hours of housing with littermates on a distinct bedding material, followed by 24 hours of housing

376 in social isolation on a different bedding material (Figure 5A). The preference of individual mice for each

377 bedding material was assessed before and after this conditioning procedure, in sessions we refer to as

378 "baseline" and "test", respectively.

379 We evaluated social CPP in littermate offspring of Oprm1+/- parents, as well as age-matched offspring

380 of Oprm1+/+ or Oprm1-/- parents (Figure 5B). There was a significant Session x Group interaction ($F_{4,112}$=3.85,

381 p=0.006, η_p^2=0.12), with significant social CPP observed in Oprm1+/+ offspring of Oprm1+/+ parents (Figure

382 5C). Social CPP was absent in Oprm1-/- offspring of Oprm1-/- parents, as previously reported (Cinque et al.,

383 2012). Social CPP was also absent in Oprm1-/- and Oprm1+/- offspring of Oprm1+/- parents, suggesting social

384 reward is diminished by either full or partial loss of Oprm1 signaling. This Oprm1 knockout mouse line shows

385 intact CPP after exposure to MDMA (Robledo et al., 2004) and cocaine (Contarino et al., 2002; Nguyen et al.,

386 2012), suggesting the lack of social CPP is not due to a generalized learning or memory deficit. In addition,

387 Oprm1 copy number did not significantly influence social approach or memory in a standard three-chamber

388 test (Table 2). These results provide initial evidence for dissociable mechanisms underlying social approach

389 and social reward.

14

390   Somewhat surprisingly, Oprm1+/+ offspring of Oprm1+/- parents also failed to exhibit social CPP, even

391   though Oprm1+/+ offspring of Oprm1+/+ parents showed robust CPP (Figure 5C). While this difference could

392   theoretically be related to parental genotype, cross-fostering experiments have shown that parental care by

393   Oprm1 mutants does not alter social behavior of Oprm1+/+ mice (Becker et al., 2014). A more likely

394   explanation is that Oprm1+/+ offspring of Oprm1+/- parents were conditioned with Oprm1+/- and Oprm1-/-

395   littermates. The abnormal social behavior of mutant littermates could thus have reduced the preference for

396   social bedding that developed in Oprm1+/+ mice in a reciprocal fashion.

397

398   **Oprm1 Copy Number Alters Reciprocal Social Interaction**

399   We further evaluated reciprocal social interaction between two freely moving age- and sex-matched

400   mice: one mutant animal generated by the Oprm1 breeding strategies described above, and a novel stimulus

401   mouse that was either a mutant mouse of the same genotype or a C57Bl/6J wild-type (Figure 6A). The total

402   time spent in social interaction (mean +/- SEM) was similar for Oprm1+/+ mice interacting with Oprm1+/+ (31.0

403   +/- 2.3 s) or C57Bl/6J (25.2 +/- 3.4 s), and for Oprm1-/- mice interacting with Oprm1-/- (17.4 +/- 1.6 s) or

404   C57Bl/6J (18.4 +/- 1.5 s), so data are pooled for presentation (Figure 6B). There was a main effect of

405   Genotype ($F_{2,166}=12.31$, $p<0.01$, $\eta_p^2=0.13$), indicating both Oprm1+/- and Oprm1-/- mutants spent less time

406   than Oprm1+/+ controls engaging in social interaction. Total interaction time was also lower in female mice

407   than male mice (main effect of Sex: $F_{1,166}=10.54$, $p<0.01$, $\eta_p^2=0.06$). In this assay, breeding strategy did not

408   appear to influence social behavior: the duration of social interaction (mean +/- SEM) was similar in Oprm1+/+

409   mice whose parents were Oprm1+/+ (28.0 +/- 2.2 s) or Oprm1+/- (28.9 +/- 4.6 s), and in Oprm1-/- mice whose

410   parents were Oprm1-/- (19.1 +/- 1.85 s) or Oprm1+/- (17.0 +/- 1.4 s).

411   In the reciprocal social interaction test, the total interaction duration includes several qualitatively

412   different types of social behavior (Terranova and Laviola, 2005; Becker et al., 2014). In terms of affiliative

413   social behaviors, there was a main effect of Genotype for nose contact (Figure 6C; $F_{2,129}=3.38$, $p=0.026$,

414    $\eta_p^2=0.06$) and huddling (Figure 6D; $F_{2,129}=6.92$, $p=0.001$, $\eta_p^2=0.10$), with decreases in Oprm1-/- mutants that

415   were more moderate in Oprm1+/- mutants, relative to Oprm1+/+ controls. In terms of investigative behaviors,

416   there was a main effect of Genotype for following (Figure 6E; $F_{2,129}=8.26$, $p<0.01$, $\eta_p^2=0.11$), but no significant

15

417   change in the amount of other non-reciprocated social exploratory behaviors, such as anogenital sniffing or

418   nose-flank contact (Figure 6F).

419   In addition to the reciprocal social behavior of the mutant mouse, we also quantified social behavior of

420   the C57Bl/6J stimulus mouse in each test session. There was no difference in the total interaction duration as

421   a function of the genotype of the mutant partner (Figure 6G), but interesting trends emerged in the qualitative

422   breakdown of specific types of social behavior. In terms of affiliative social behaviors, there were similar trends

423   towards reduced nose contact and huddling, but not in following (Figure 6H-J). However, C57Bl/6J stimulus

424   mice engaged in more non-reciprocated social exploratory behaviors with Oprm1-/- mutant partners (Figure

425   6K; $F_{2,83}=3.58$, p=0.032, $\eta_p^2=0.08$). This result supports the notion that interaction with an Oprm1 mutant

426   mouse changes the social experience of genotypical test partners in a reciprocal manner.

427

428   **Oprm1 Copy Number Alters Real Time Social Preference**

429   To further assess the preference for social interaction with an Oprm1 mutant mouse versus a typical

430   Oprm1+/+ mouse, we measured the choice between these two types of social interaction in real time (Shah et

431   al., 2013). In an initial set of experiments, C57Bl/6J mice served as "judges" in a chamber with two confined

432   stimulus mice (Figure 7A). One of these stimulus mice was "typical" (Oprm1+/+ wildtype), while the other

433   stimulus mouse was "atypical" (Oprm1+/- mutant). Both stimulus mice were age- and sex-matched to the

434   judge. C57Bl/6J judges failed to exhibit reliable discrimination between atypical Oprm1+/- mutants and typical

435   Oprm1+/+ controls (Figure 7B-C). However, C57Bl/6J judges did reliably discriminate between atypical Oprm1-

436   /- mutants and typical Oprm1+/+ controls (Figure 7D-F), exhibiting a robust social preference for the chamber

437   containing the typical mouse ($F_{1,22}=5.87$, p=0.002, $\eta_p^2=0.21$). These data provide converging evidence that the

438   abnormal social behavior exhibited by Oprm1 mutant mice can negatively influence the reciprocal social

439   preference of genotypical conspecifics.

440   Since C57Bl/6J judges exhibited reliable discrimination between atypical Oprm1-/- mutants and typical

441   Oprm1+/+ controls, we used the same experimental setup to test the real time social preference of judges that

442   were Oprm1 mutants. Oprm1+/- judges failed to discriminate between atypical Oprm1-/- mutants and typical

443   Oprm1+/+ controls (Figure 7F-H). In contrast, Oprm1-/- judges did reliably discriminate between atypical

16

444 Oprm1-/- mutants and typical Oprm1+/+ controls (Figure 7I-K). However, these Oprm1-/- judges exhibited a

445 robust social preference for the chamber containing another atypical Oprm1-/- mouse ($F_{1,11}$=19.94, p=0.001,

446 η_p^2=0.64). Oprm1-/- mice did not develop social CPP when housed with other Oprm1-/- mice (Figure 5),

447 providing further evidence for dissociable mechanisms underlying social approach and social reward. Our

448 results link deficits in mu opioid receptor signaling with impairment of social reward, rather than social

449 approach, and illustrate how social interaction with Oprm1 mutant mice can affect behavior of genotypical

450 partners in a reciprocal fashion.

451

452 **DISCUSSION**

453 Dysregulation of mu opioid receptor signaling has been reported in a variety of neuropsychiatric

454 disorders that involve altered social behavior (Kennedy et al., 2006; Prossin et al., 2010; Pellissier et al., 2018;

455 Ashok et al., 2019; Nummenmaa et al., 2020). These conditions likely involve a partial (rather than complete)

456 dysregulation of mu opioid receptor signaling, which we have modeled using mice with heterozygous genetic

457 knockout of Oprm1. These mice exhibited changes in the organization of inhibitory microcircuitry within the

458 nucleus accumbens, where mu opioid receptor activation plays a particularly critical role in social behavior.

459 Haploinsufficiency of mu opioid receptor signaling led to robust deficits in both social CPP and reciprocal social

460 interaction in Oprm1+/- mice. Furthermore, the reciprocal social behavior of genotypical stimulus mice was

461 also affected by interaction with Oprm1 mutant mice, which represents a novel aspect of social impairments

462 caused by deficient mu opioid receptor signaling. Partial reductions of mu opioid receptor signaling can thus

463 have wide-ranging impacts on both neural circuit organization and behavioral output.

464

465 **Oprm1 Copy Number and Remodeling of Nucleus Accumbens Microcircuitry**

466 The mu opioid receptor is abundant in the nucleus accumbens (Moskowitz and Goodman, 1984), and

467 its activation can bidirectionally modulate social preference in rodents (Trezza et al., 2011; Resendez et al.,

468 2013; Smith et al., 2018). Homozygous Oprm1 knockout mice also show a dramatic increase in the number of

469 symmetrical synapses within the nucleus accumbens (Becker et al., 2014). We corroborated this prior report by

470 measuring mRNA expression of inhibitory synaptic molecules, and using gephyrin immunoreactivity as a

17

471   marker of perisomatic inhibitory synapses onto D2-MSNs. The density of gephyrin puncta was significantly

472   elevated in Oprm1-/- mice, and elevated even further in Oprm1+/- mice, with no evidence of a sex difference.

473   This striking data show haploinsufficiency of mu opioid receptor gene expression can cause more dramatic

474   neurobiological changes than complete genetic knockout of Oprm1, perhaps due to compensatory adaptations

475   that occur in the total absence of mu opioid receptor expression.

476   In male Oprm1+/- mice, the structural reorganization of inhibitory synapses onto D2-MSNs was

477   accompanied by altered inhibitory synaptic transmission. There was a significant increase in mIPSC amplitude

478   and frequency in D2-MSNs from male Oprm1+/- mice, similar to previous observations in the central amygdala

479   of male Oprm1-/- mice (Kang-Park et al., 2009). The increase in mIPSC frequency was particularly pronounced

480   for events of large amplitude, which likely correspond to the perisomatic synapses detected using gephyrin

481   immunoreactivity. Fast-spiking interneurons tend to form perisomatic inhibitory synapses with large quantal

482   amplitude onto striatal MSNs (Straub et al., 2016), and these interneurons express the mu opioid receptor in

483   other brain regions (Drake and Milner, 2006; Glickfeld et al., 2008; Krook-Magnuson et al., 2011). This raises

484   the possibility that loss of mu opioid receptor expression from presynaptic neurons may contribute to

485   remodeling of inhibitory synapses onto MSNs in male mice, although the mu opioid receptor is also expressed

486   by postsynaptic MSNs (Banghart et al., 2015; Charbogne et al., 2017). Additional research is needed to

487   determine whether inhibitory microcircuits are regulated by mu opioid receptor expression in specific nucleus

488   accumbens cell types, as previously shown for responses to exogenous opioid exposure (Cui et al., 2014;

489   Charbogne et al., 2017; Severino et al., 2020).

490   Paradoxically, functional changes in synaptic transmission were not observed in female Oprm1+/- mice,

491   even though both sexes showed a comparable increase in D2-MSN gephyrin puncta density and gephyrin

492   mRNA expression. One potential explanation for this pattern of results is that the basal mIPSC amplitude is

493   higher in D2-MSNs of female mice and D1-MSNs of male mice. A ceiling effect may therefore have obscured

494   our ability to detect increased mIPSC amplitude in D2-MSNs from female Oprm1 mutant mice. While sex

495   differences at nucleus accumbens inhibitory synapses have not previously been investigated in a cell type-

496   specific fashion, there are well-documented sex differences in the structure and function of excitatory synapses

497   in the nucleus accumbens (Forlano and Woolley, 2010; Meitzen et al., 2018), including cell type-specific

18

498 changes (Cao et al., 2018). We did not detect changes in the mRNA expression of excitatory synaptic

499 scaffolding molecules, and thus did not further evaluate excitatory synaptic transmission in this study. Since

500 inhibitory synaptic transmission appeared relatively normal in female Oprm1-/- mice, changes in excitatory

501 synaptic transmission could make a larger contribution to their atypical social behavior. However, both sexes

502 showed robust changes in gephyrin mRNA expression and D2-MSN gephyrin puncta density, suggesting a

503 common reorganization of inhibitory microcircuitry caused by complete or partial decrements in mu opioid

504 receptor signaling. It is noteworthy that reductions in sociability caused by social defeat stress are associated

505 with decreased mIPSC frequency in the nucleus accumbens (Heshmati et al., 2020), but this may be due to an

506 effect on D1-MSNs rather than D2-MSNs (Heshmati et al., 2018).

507

508 **Multifaceted Influence of Oprm1 Copy Number on Reciprocal Social Behavior**

509 Homozygous Oprm1 knockout mice have deficits in maternal attachment (Moles et al., 2004), social

510 reward (Cinque et al., 2012), and reciprocal social interaction (Becker et al., 2014). We extended these

511 analyses to Oprm1+/- mice using a breeding strategy that permitted comparison with both Oprm1+/+ and

512 Oprm1-/- littermates, as well as Oprm1+/+ and Oprm1-/- offspring of parents with the same genotype. We

513 found that Oprm1+/- mice had significant reductions in the time spent interacting with novel conspecifics in the

514 reciprocal social interaction test, similar to the phenotype we and others observed in Oprm1-/- mice (Becker et

515 al., 2014). We also analyzed the behavior of genotypical stimulus mice tested with Oprm1 mutant partners in

516 the reciprocal social interaction test. We found subtle indications that interaction with Oprm1 mutant mice alters

517 the reciprocal social behavior of genotypical stimulus mice, as previously reported for other mouse strains with

518 atypical social behavior (Yang et al., 2012).

519 This notion was further supported by two additional lines of evidence. First, in a test of social CPP, the

520 preference normally observed for group housing with conspecifics was absent when Oprm1+/+ mice were

521 housed with Oprm1 mutant littermates. Second, in a test of real time social preference (Shah et al., 2013),

522 genotypical judges exhibited a preference for interaction with typical Oprm1+/+ mice versus atypical Oprm1-/-

523 mice. This preference was not observed when the atypical mouse was Oprm1+/-, so heterozygous deletion of

524 the mu opioid receptor does not completely recapitulate all social phenotypes of homozygous Oprm1 knockout

19

525 mice. Our findings are consistent with other reports that social behavior of genotypical mice can be influenced

526 by atypical conspecifics (Langford et al., 2010; Yang et al., 2012; Heinla et al., 2018; Rogers-Carter et al.,

527 2018).

528   To our surprise, when Oprm1-/- served as judges in the real time social preference test, they exhibited

529 a preference for other Oprm1-/- mice rather than "typical" Oprm1+/+ mice. We also found that Oprm1-/-

530 exhibited normal levels of social approach in a three-chamber social test (Nadler et al., 2004). These findings

531 differ somewhat from a previous study of the same Oprm1 knockout mouse on a different genetic background

532 (Becker et al., 2014), but genetic background is known to influence behavior in the three-chamber social test

533 (Moy et al., 2004). It is notable that Oprm1-/- do not develop social CPP when housed with other Oprm1-/-

534 littermates (Cinque et al., 2012). This suggests that Oprm1-/- mutants may not enjoy or "like" social interaction

535 with other Oprm1-/- mutants, but still pursue or "want" such interaction. A role for opioid signaling in the

536 hedonic impact of social interaction is consistent with prominent theories of reward (Berridge et al., 2009),

537 which conversely predict that dopamine signaling may mediate pursuit of social interaction (Gunaydin et al.,

538 2014).

539

540 **Translational Implications**

541   Our findings demonstrate that partial disruption of mu opioid receptor signaling can have profound

542 effects on both neural circuit organization and behavioral output. In some cases, the impact of

543 haploinsufficiency was even greater than complete loss of mu opioid receptor signaling. The dysregulation of

544 mu opioid receptor signaling reported in a variety of neuropsychiatric disorders may therefore reflect

545 fundamental alterations in brain function, and contribute to the pathophysiology of these conditions (Kennedy

546 et al., 2006; Prossin et al., 2010; Pellissier et al., 2018; Ashok et al., 2019; Nummenmaa et al., 2020). Partial

547 loss of mu opioid receptor signaling could be caused by genetic polymorphisms affecting the receptor itself,

548 associated signaling proteins, and opioid peptide ligands as well as their catabolic enzymes. Conversely,

549 genetic variants that enhance some aspects of mu opioid receptor signaling (like the Oprm1 A118G

550 polymorphism) can increase sociability, even in the heterozygous state (Barr et al., 2008; Copeland et al.,

551 2011; Troisi et al., 2011; Briand et al., 2015). A similar enhancement of endogenous opioid signaling may be

20

552 possible via pharmacological inhibition of the enzymes that normally degrade endogenous opioid peptides

553 (Roques et al., 2012), or through positive allosteric modulation of the mu opioid receptor (Kandasamy et al.,

554 2021). Therefore, signaling via the mu opioid receptor may not only contribute to the etiology of

555 neuropsychiatric disorders, but also represent a target for therapeutic intervention.

556

557 **REFERENCES**

558

559 Achterberg EJM, van Swieten MMH, Houwing DJ, Trezza V, Vanderschuren L (2019) Opioid modulation of
560   social play reward in juvenile rats. Neuropharmacology 159:107332.

561 Aragona BJ, Liu Y, Yu YJ, Curtis JT, Detwiler JM, Insel TR, Wang Z (2006) Nucleus accumbens dopamine
562   differentially mediates the formation and maintenance of monogamous pair bonds. Nat Neurosci 9:133-139.

563 Ashok AH, Myers J, Reis Marques T, Rabiner EA, Howes OD (2019) Reduced mu opioid receptor availability
564   in schizophrenia revealed with [(11)C]-carfentanil positron emission tomographic Imaging. Nat Commun
565   10:4493.

566 Baldo BA, Kelley AE (2007) Discrete neurochemical coding of distinguishable motivational processes: insights
567   from nucleus accumbens control of feeding. Psychopharmacology (Berl) 191:439-459.

568 Banghart MR, Neufeld SQ, Wong NC, Sabatini BL (2015) Enkephalin Disinhibits Mu Opioid Receptor-Rich
569   Striatal Patches via Delta Opioid Receptors. Neuron 88:1227-1239.

570 Banovic D, Khorramshahi O, Owald D, Wichmann C, Riedt T, Fouquet W, Tian R, Sigrist SJ, Aberle H (2010)
571   Drosophila neuroligin 1 promotes growth and postsynaptic differentiation at glutamatergic neuromuscular
572   junctions. Neuron 66:724-738.

573 Barr CS, Schwandt ML, Lindell SG, Higley JD, Maestripieri D, Goldman D, Suomi SJ, Heilig M (2008) Variation
574   at the mu-opioid receptor gene (OPRM1) influences attachment behavior in infant primates. Proc Natl Acad
575   Sci U S A 105:5277-5281.

576 Becker JA, Clesse D, Spiegelhalter C, Schwab Y, Le Merrer J, Kieffer BL (2014) Autistic-like syndrome in mu
577   opioid receptor null mice is relieved by facilitated mGluR4 activity. Neuropsychopharmacology 39:2049-
578   2060.

579 Berridge KC, Robinson TE, Aldridge JW (2009) Dissecting components of reward: 'liking', 'wanting', and
580   learning. Curr Opin Pharmacol 9:65-73.

581 Briand LA, Hilario M, Dow HC, Brodkin ES, Blendy JA, Berton O (2015) Mouse model of OPRM1 (A118G)
582   polymorphism increases sociability and dominance and confers resilience to social defeat. J Neurosci
583   35:3582-3590.

584 Cao J, Dorris DM, Meitzen J (2018) Electrophysiological properties of medium spiny neurons in the nucleus
585   accumbens core of prepubertal male and female Drd1a-tdTomato line 6 BAC transgenic mice. J
586   Neurophysiol 120:1712-1727.

587 Castro DC, Bruchas MR (2019) A Motivational and Neuropeptidergic Hub: Anatomical and Functional Diversity
588   within the Nucleus Accumbens Shell. Neuron 102:529-552.

589 Charbogne P et al. (2017) Mu Opioid Receptors in Gamma-Aminobutyric Acidergic Forebrain Neurons
590   Moderate Motivation for Heroin and Palatable Food. Biol Psychiatry 81:778-788.

591 Chelnokova O, Laeng B, Løseth G, Eikemo M, Willoch F, Leknes S (2016) The μ-opioid system promotes
592   visual attention to faces and eyes. Social cognitive and affective neuroscience 11:1902-1909.

593 Chen X, Liu Z, Ma C, Ma L, Liu X (2019) Parvalbumin Interneurons Determine Emotional Valence Through
594   Modulating Accumbal Output Pathways. Front Behav Neurosci 13:110.

595 Cinque C, Pondiki S, Oddi D, Di Certo MG, Marinelli S, Troisi A, Moles A, D'Amato FR (2012) Modeling
596   socially anhedonic syndromes: genetic and pharmacological manipulation of opioid neurotransmission in
597   mice. Transl Psychiatry 2:e155.

598 Contarino A, Picetti R, Matthes HW, Koob GF, Kieffer BL, Gold LH (2002) Lack of reward and locomotor
599   stimulation induced by heroin in mu-opioid receptor-deficient mice. Eur J Pharmacol 446:103-109.

600 Copeland WE, Sun H, Costello EJ, Angold A, Heilig MA, Barr CS (2011) Child mu-opioid receptor gene variant
601   influences parent-child relations. Neuropsychopharmacology 36:1165-1170.

602 Cui Y, Ostlund SB, James AS, Park CS, Ge W, Roberts KW, Mittal N, Murphy NP, Cepeda C, Kieffer BL,
603   Levine MS, Jentsch JD, Walwyn WM, Sun YE, Evans CJ, Maidment NT, Yang XW (2014) Targeted
604   expression of mu-opioid receptors in a subset of striatal direct-pathway neurons restores opiate reward. Nat
605   Neurosci 17:254-261.

606 Darcq E, Kieffer BL (2018) Opioid receptors: drivers to addiction? Nat Rev Neurosci 19:499-514.

607 Dolen G, Darvishzadeh A, Huang KW, Malenka RC (2013) Social reward requires coordinated activity of
608   nucleus accumbens oxytocin and serotonin. Nature 501:179-184.

609 Drake CT, Milner TA (2006) Mu opioid receptors are extensively co-localized with parvalbumin, but not
610   somatostatin, in the dentate gyrus. Neurosci Lett 403:176-180.

611 Forlano PM, Woolley CS (2010) Quantitative analysis of pre- and postsynaptic sex differences in the nucleus
612   accumbens. J Comp Neurol 518:1330-1348.

613 Gittis AH, Hang GB, LaDow ES, Shoenfeld LR, Atallah BV, Finkbeiner S, Kreitzer AC (2011) Rapid target-
614   specific remodeling of fast-spiking inhibitory circuits after loss of dopamine. Neuron 71:858-868.

615 Glickfeld LL, Atallah BV, Scanziani M (2008) Complementary modulation of somatic inhibition by opioids and
616   cannabinoids. J Neurosci 28:1824-1832.

617 Gong S, Zheng C, Doughty ML, Losos K, Didkovsky N, Schambra UB, Nowak NJ, Joyner A, Leblanc G, Hatten
618   ME, Heintz N (2003) A gene expression atlas of the central nervous system based on bacterial artificial
619   chromosomes. Nature 425:917-925.

620 Guard HJ, Newman JD, Roberts RL (2002) Morphine administration selectively facilitates social play in
621   common marmosets. Dev Psychobiol 41:37-49.

622 Gunaydin LA, Grosenick L, Finkelstein JC, Kauvar IV, Fenno LE, Adhikari A, Lammel S, Mirzabekov JJ, Airan
623   RD, Zalocusky KA, Tye KM, Anikeeva P, Malenka RC, Deisseroth K (2014) Natural neural projection
624   dynamics underlying social behavior. Cell 157:1535-1551.

625 Heinla I, Ahlgren J, Vasar E, Voikar V (2018) Behavioural characterization of C57BL/6N and BALB/c female
626   mice in social home cage - Effect of mixed housing in complex environment. Physiol Behav 188:32-41.

627 Heshmati M, Christoffel DJ, LeClair K, Cathomas F, Golden SA, Aleyasin H, Turecki G, Friedman AK, Han MH,
628   Menard C, Russo SJ (2020) Depression and Social Defeat Stress Are Associated with Inhibitory Synaptic
629   Changes in the Nucleus Accumbens. J Neurosci 40:6228-6233.

630 Heshmati M, Aleyasin H, Menard C, Christoffel DJ, Flanigan ME, Pfau ML, Hodes GE, Lepack AE, Bicks LK,
631   Takahashi A, Chandra R, Turecki G, Lobo MK, Maze I, Golden SA, Russo SJ (2018) Cell-type-specific role
632   for nucleus accumbens neuroligin-2 in depression and stress susceptibility. Proc Natl Acad Sci U S A
633   115:1111-1116.

23

634 Hsu DT, Sanford BJ, Meyers KK, Love TM, Hazlett KE, Walker SJ, Mickey BJ, Koeppe RA, Langenecker SA,
635   Zubieta JK (2015) It still hurts: altered endogenous opioid activity in the brain during social rejection and
636   acceptance in major depressive disorder. Molecular psychiatry 20:193-200.

637 Hsu DT, Sanford BJ, Meyers KK, Love TM, Hazlett KE, Wang H, Ni L, Walker SJ, Mickey BJ, Korycinski ST,
638   Koeppe RA, Crocker JK, Langenecker SA, Zubieta JK (2013) Response of the µ-opioid system to social
639   rejection and acceptance. Molecular psychiatry 18:1211-1217.

640 Kandasamy R, Hillhouse TM, Livingston KE, Kochan KE, Meurice C, Eans SO, Li MH, White AD, Roques BP,
641   McLaughlin JP, Ingram SL, Burford NT, Alt A, Traynor JR (2021) Positive allosteric modulation of the mu-
642   opioid receptor produces analgesia with reduced side effects. Proc Natl Acad Sci U S A 118.

643 Kang-Park MH, Kieffer BL, Roberts AJ, Roberto M, Madamba SG, Siggins GR, Moore SD (2009) Mu-opioid
644   receptors selectively regulate basal inhibitory transmission in the central amygdala: lack of ethanol
645   interactions. J Pharmacol Exp Ther 328:284-293.

646 Kennedy SE, Koeppe RA, Young EA, Zubieta JK (2006) Dysregulation of endogenous opioid emotion
647   regulation circuitry in major depression in women. Arch Gen Psychiatry 63:1199-1208.

648 Kieffer BL, Gaveriaux-Ruff C (2002) Exploring the opioid system by gene knockout. Prog Neurobiol 66:285-
649   306.

650 Kins S, Betz H, Kirsch J (2000) Collybistin, a newly identified brain-specific GEF, induces submembrane
651   clustering of gephyrin. Nat Neurosci 3:22-29.

652 Koos T, Tepper JM, Wilson CJ (2004) Comparison of IPSCs evoked by spiny and fast-spiking neurons in the
653   neostriatum. J Neurosci 24:7916-7922.

654 Krook-Magnuson E, Luu L, Lee SH, Varga C, Soltesz I (2011) Ivy and neurogliaform interneurons are a major
655   target of mu-opioid receptor modulation. J Neurosci 31:14861-14870.

656 Langford DJ, Tuttle AH, Brown K, Deschenes S, Fischer DB, Mutso A, Root KC, Sotocinal SG, Stern MA,
657   Mogil JS, Sternberg WF (2010) Social approach to pain in laboratory mice. Soc Neurosci 5:163-170.

658 Lefevre EM, Pisansky MT, Toddes C, Baruffaldi F, Pravetoni M, Tian L, Kono TJY, Rothwell PE (2020)
659   Interruption of continuous opioid exposure exacerbates drug-evoked adaptations in the mesolimbic
660   dopamine system. Neuropsychopharmacology.

661 Manduca A, Servadio M, Damsteegt R, Campolongo P, Vanderschuren LJ, Trezza V (2016) Dopaminergic
662   Neurotransmission in the Nucleus Accumbens Modulates Social Play Behavior in Rats.
663   Neuropsychopharmacology 41:2215-2223.

664 Matthes HWD, Maldonado R, Simonin F, Valverde O, Slowe S, Kitchen I, Befort K, Dierich A, Le Meur M, Dolie
665   P, Tzavara E, Hanoune J, Roques BP, Kieffer BL (1996) Loss of morphine-induced analgesia, reward effect
666   and withdrawal symptoms in mice lacking the µ-opioid-receptor gene. Nature 383:822-823.

667 Meitzen J, Meisel RL, Mermelstein PG (2018) Sex Differences and the Effects of Estradiol on Striatal Function.
668   Curr Opin Behav Sci 23:42-48.

669 Moles A, Kieffer BL, D'Amato FR (2004) Deficit in attachment behavior in mice lacking the mu-opioid receptor
670   gene. Science 304:1983-1986.

671 Moskowitz AS, Goodman RR (1984) Light microscopic autoradiographic localization of mu and delta opioid
672   binding sites in the mouse central nervous system. J Neurosci 4:1331-1342.

673   Nadler JJ, Moy SS, Dold G, Trang D, Simmons N, Perez A, Young NB, Barbaro RP, Piven J, Magnuson TR,
674   Crawley JN (2004) Automated apparatus for quantitation of social approach behaviors in mice. Genes Brain
675   Behav 3:303-314.

676   Nguyen AT, Marquez P, Hamid A, Kieffer B, Friedman TC, Lutfy K (2012) The rewarding action of acute
677   cocaine is reduced in beta-endorphin deficient but not in mu opioid receptor knockout mice. Eur J
678   Pharmacol 686:50-54.

679   Nummenmaa L, Karjalainen T, Isojarvi J, Kantonen T, Tuisku J, Kaasinen V, Joutsa J, Nuutila P, Kalliokoski K,
680   Hirvonen J, Hietala J, Rinne J (2020) Lowered endogenous mu-opioid receptor availability in subclinical
681   depression and anxiety. Neuropsychopharmacology.

682   Panksepp J, Herman BH, Vilberg T, Bishop P, DeEskinazi FG (1980) Endogenous opioids and social behavior.
683   Neuroscience and Biobehavioral Reviews 4:473-487.

684   Panksepp JB, Lahvis GP (2007) Social reward among juvenile mice. Genes Brain Behav 6:661-671.

685   Pellissier LP, Gandía J, Laboute T, Becker JAJ, Le Merrer J (2018) µ opioid receptor, social behaviour and
686   autism spectrum disorder: reward matters. British Journal of Pharmacology 175:2750-2769.

687   Pisansky MT, Lefevre EM, Retzlaff CL, Trieu BH, Leipold DW, Rothwell PE (2019) Nucleus Accumbens Fast-
688   Spiking Interneurons Constrain Impulsive Action. Biol Psychiatry 86:836-847.

689   Prossin AR, Love TM, Koeppe RA, Zubieta JK, Silk KR (2010) Dysregulation of regional endogenous opioid
690   function in borderline personality disorder. Am J Psychiatry 167:925-933.

691   Resendez SL, Dome M, Gormley G, Franco D, Nevárez N, Hamid AA, Aragona BJ (2013) µ-Opioid receptors
692   within subregions of the striatum mediate pair bond formation through parallel yet distinct reward
693   mechanisms. Journal of Neuroscience 33:9140-9149.

694   Richard JM, Castro DC, Difeliceantonio AG, Robinson MJ, Berridge KC (2013) Mapping brain circuits of
695   reward and motivation: in the footsteps of Ann Kelley. Neurosci Biobehav Rev 37:1919-1931.

696   Robledo P, Mendizabal V, Ortuno J, de la Torre R, Kieffer BL, Maldonado R (2004) The rewarding properties
697   of MDMA are preserved in mice lacking mu-opioid receptors. Eur J Neurosci 20:853-858.

698   Rogers-Carter MM, Varela JA, Gribbons KB, Pierce AF, McGoey MT, Ritchey M, Christianson JP (2018)
699   Insular cortex mediates approach and avoidance responses to social affective stimuli. Nat Neurosci 21:404-
700   414.

701   Roques BP, Fournie-Zaluski MC, Wurm M (2012) Inhibiting the breakdown of endogenous opioids and
702   cannabinoids to alleviate pain. Nat Rev Drug Discov 11:292-310.

703   Severino AL, Mittal N, Hakimian JK, Velarde N, Minasyan A, Albert R, Torres C, Romaneschi N, Johnston C,
704   Tiwari S, Lee AS, Taylor AM, Gaveriaux-Ruff C, Kieffer BL, Evans CJ, Cahill CM, Walwyn WM (2020) mu-
705   Opioid Receptors on Distinct Neuronal Populations Mediate Different Aspects of Opioid Reward-Related
706   Behaviors. eNeuro 7.

707   Shah CR, Forsberg CG, Kang JQ, Veenstra-Vanderweele J (2013) Letting a Typical Mouse Judge Whether
708   Mouse Social Interactions Are Atypical. Autism Research 6:212-220.

709   Shuen JA, Chen M, Gloss B, Calakos N (2008) Drd1a-tdTomato BAC transgenic mice for simultaneous
710   visualization of medium spiny neurons in the direct and indirect pathways of the basal ganglia. J Neurosci
711   28:2681-2685.

25

712 Smith CJW, Wilkins KB, Li S, Tulimieri MT, Veenema AH (2018) Nucleus accumbens mu opioid receptors
713   regulate context-specific social preferences in the juvenile rat. Psychoneuroendocrinology 89:59-68.

714 Sora I, Elmer G, Funada M, Pieper J, Li XF, Hall FS, Uhl GR (2001) Mu opiate receptor gene dose effects on
715   different morphine actions: evidence for differential in vivo mu receptor reserve. Neuropsychopharmacology
716   25:41-54.

717 Straub C, Saulnier JL, Begue A, Feng DD, Huang KW, Sabatini BL (2016) Principles of Synaptic Organization
718   of GABAergic Interneurons in the Striatum. Neuron 92:84-92.

719 Terranova ML, Laviola G (2005) Scoring of social interactions and play in mice during adolescence. Curr
720   Protoc Toxicol Chapter 13:Unit13 10.

721 Trezza V, Baarendse PJJ, Vanderschuren LJMJ (2010) The pleasures of play: pharmacological insights into
722   social reward mechanisms. Trends in pharmacological sciences 31:463-469.

723 Trezza V, Damsteegt R, Achterberg EJ, Vanderschuren LJ (2011) Nucleus accumbens mu-opioid receptors
724   mediate social reward. J Neurosci 31:6362-6370.

725 Troisi A, Frazzetto G, Carola V, Di Lorenzo G, Coviello M, D'Amato FR, Moles A, Siracusano A, Gross C
726   (2011) Social hedonic capacity is associated with the A118G polymorphism of the mu-opioid receptor gene
727   (OPRM1) in adult healthy volunteers and psychiatric patients. Soc Neurosci 6:88-97.

728 Tyagarajan SK, Fritschy JM (2014) Gephyrin: a master regulator of neuronal function? Nat Rev Neurosci
729   15:141-156.

730 Wang X, Gallegos DA, Pogorelov VM, O'Hare JK, Calakos N, Wetsel WC, West AE (2018) Parvalbumin
731   Interneurons of the Mouse Nucleus Accumbens are Required For Amphetamine-Induced Locomotor
732   Sensitization and Conditioned Place Preference. Neuropsychopharmacology 43:953-963.

733 Won S, Levy JM, Nicoll RA, Roche KW (2017) MAGUKs: multifaceted synaptic organizers. Curr Opin
734   Neurobiol 43:94-101.

735 Yang M, Abrams DN, Zhang JY, Weber MD, Katz AM, Clarke AM, Silverman JL, Crawley JN (2012) Low
736   sociability in BTBR T+tf/J mice is independent of partner strain. Physiol Behav 107:649-662.
737
738

739 **FIGURES AND FIGURE LEGENDS**
740
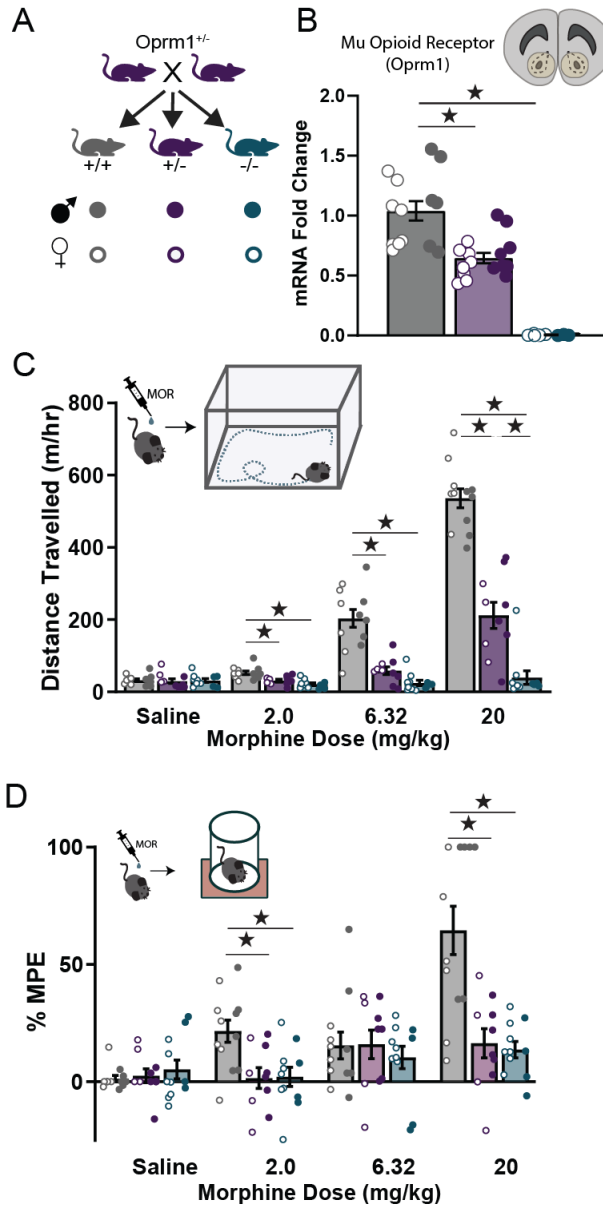
741
742
743 **Figure 1. Functional validation of Oprm1 haploinsufficiency. (A)** Breeding strategy used to generate
744 littermates of all possible genotypes for validation experiments (top), with legend defining appearance of
745 individual data points for each genotype and sex (bottom). **(B)** Assessment of mu opioid receptor (Oprm1)
746 mRNA levels in nucleus accumbens tissue punches using quantitative PCR in Oprm1+/+ (n=14), Oprm1+/-
747 (n=15), and Oprm1-/- (n=9). **(C-D)** Distance travelled in a test of open field activity (C) and thermal
748 antinociception on the hot plate (D) after injection of morphine in Oprm1+/+ (n=12), Oprm1+/- (n=10), and
749 Oprm1-/- (n=11). All groups contained similar numbers of female mice (open symbols) and male mice (closed
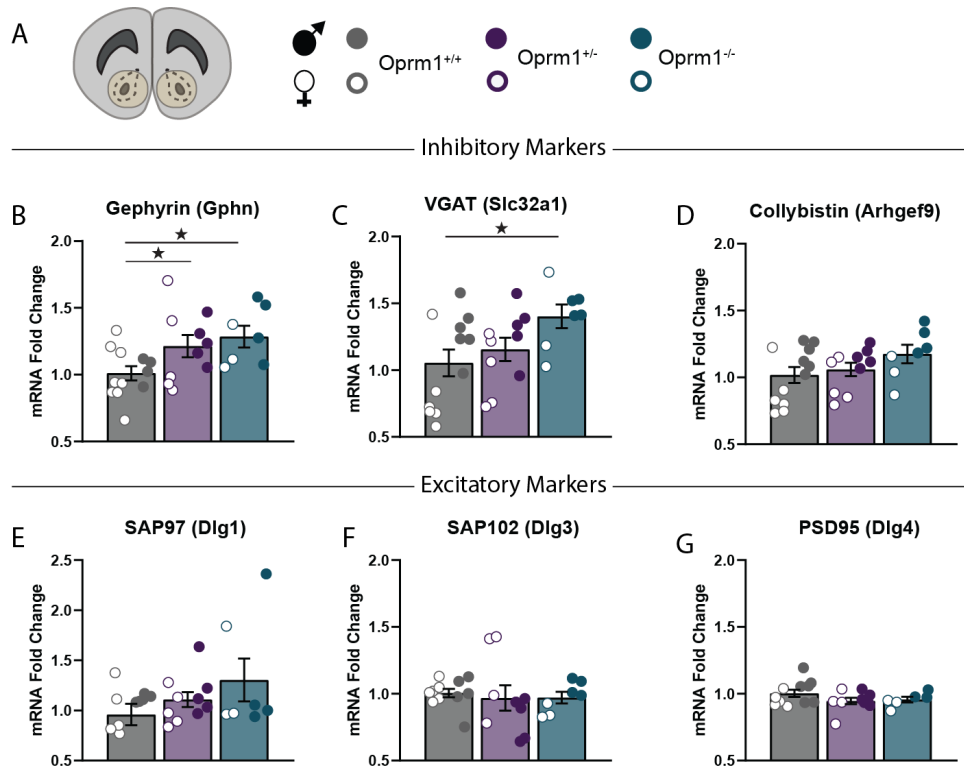750 symbols); *p<0.05 between groups, LSD post-hoc test.

27

751
752
753 **Figure 2. Oprm1 copy number affects synaptic gene expression in the nucleus accumbens. (A)**
754 Assessment of mRNA levels in nucleus accumbens tissue punches using quantitative PCR (left), with figure
755 legend (right) for Oprm1+/+ (n=12), Oprm1+/- (n=10), and Oprm1-/- (n=7). **(B-D)** Expression of inhibitory
756 synaptic genes: gephyrin (B), vesicular GABA transporter (VGAT; C), and collybistin (D). **(E-G)** Expression of
757 excitatory synaptic genes: SAP97 (E), SAP102 (F), and PSD95 (G). All groups contained similar numbers of
758 female mice (open symbols) and male mice (closed symbols); *p<0.05 between groups, LSD post-hoc test.
759

28
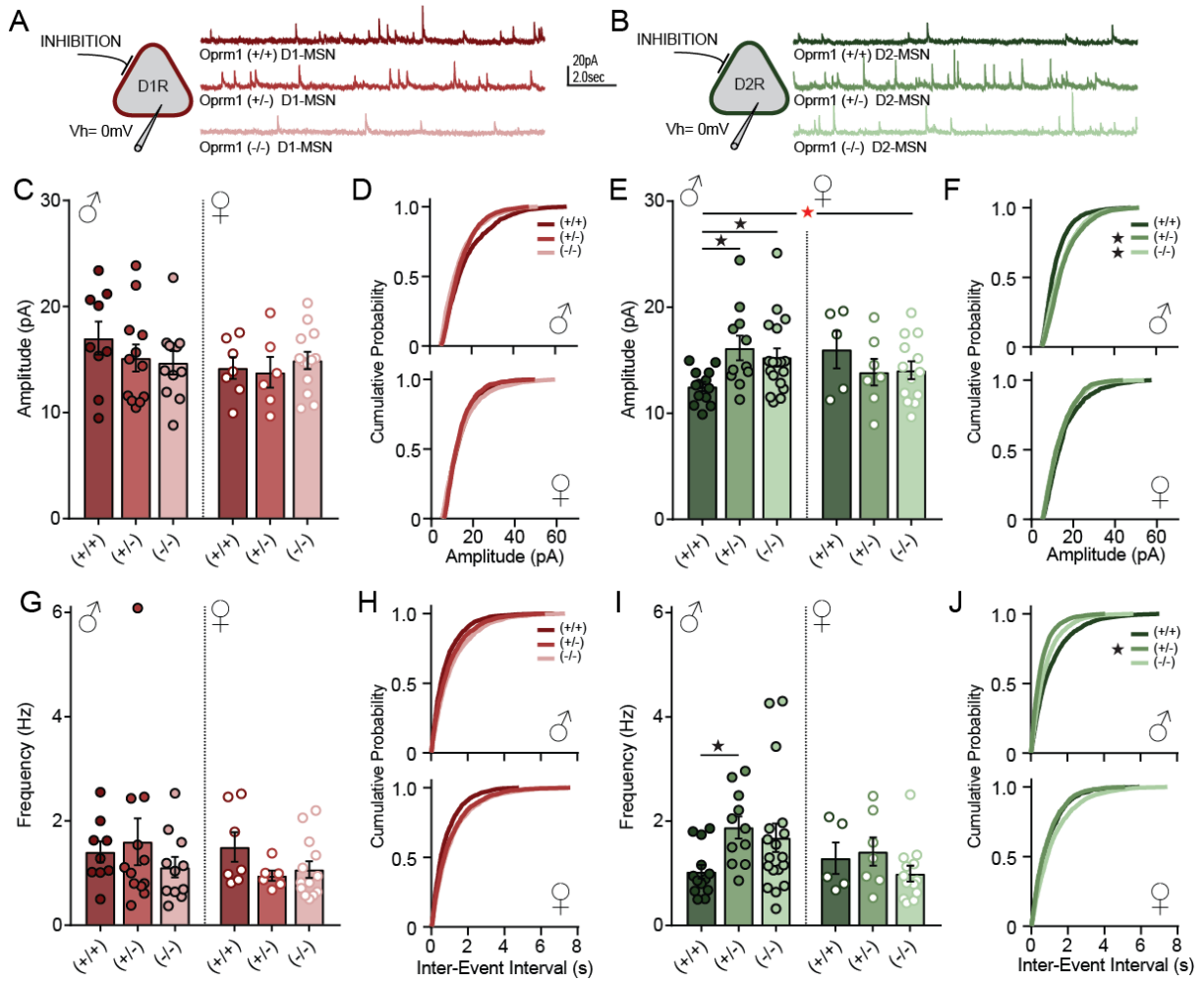
Figure 3. Electrophysiological recordings from medium spiny projection neurons (MSNs) in the nucleus accumbens, to assess inhibitory synaptic transmission. (A-B) Schematic diagram showing whole-cell voltage-clamp recordings from MSNs identified by expression of Drd1-tdTomato (A) or Drd2-eGFP (B). Example traces show miniature inhibitory postsynaptic currents (mIPSCs) recorded for Oprm1+/+ (n=16/18 cells for D1/D2), Oprm1+/- (n=18/18 for D1/D2), and Oprm1-/- (n=24/31 cells of D1/D2). **(C-F)** Average mIPSC amplitude and cumulative probability plots for D1-MSNs (C-D) and D2-MSNs (E-F), separated by sex. **(G-J)** Average mIPSC frequency and cumulative probability plots for D1-MSNs (G-H**)** and D2-MSNs (I-J), separated by sex. Red asterisk indicates a significant Genotype x Sex interaction (E); *p<0.05 according to LSD post-hoc test (E, I) or Kolmogorov-Smirnov test comparing Oprm1 mutant to control (F, J).
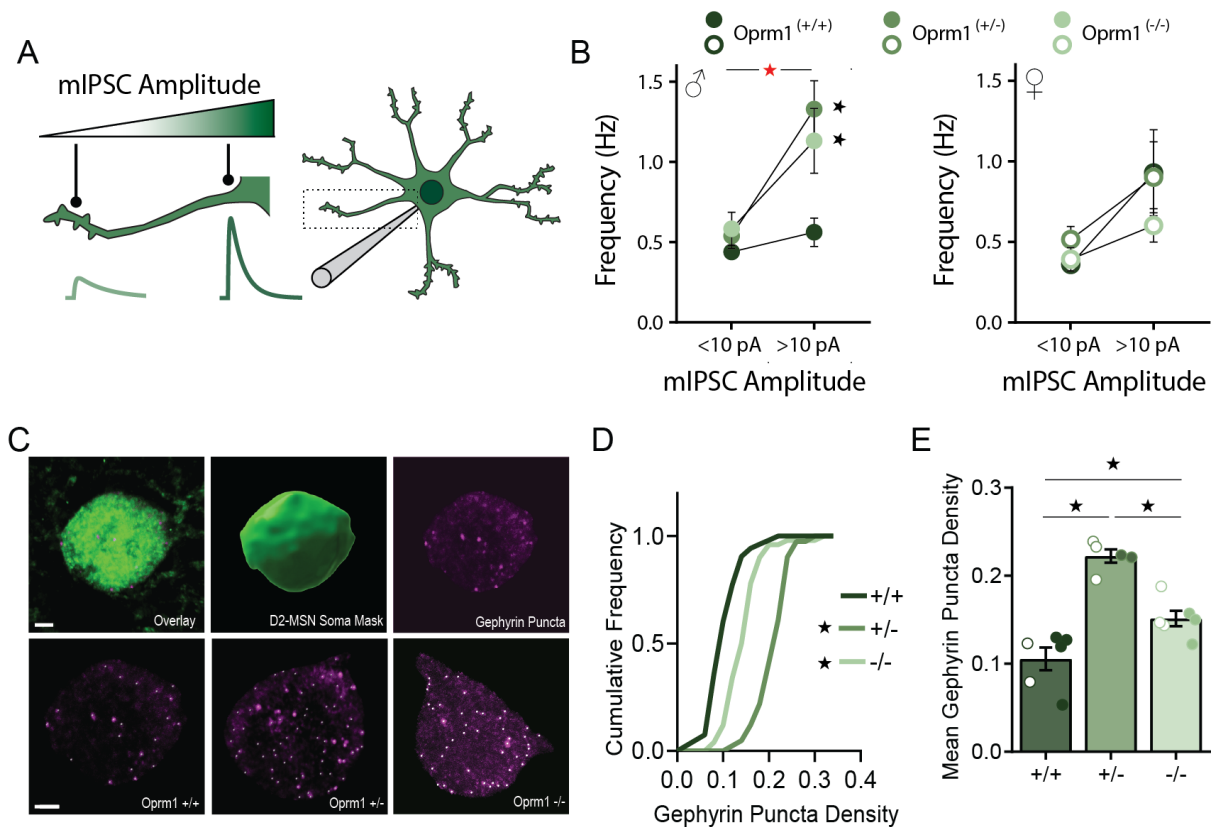
Figure 4. Functional and structural analysis of perisomatic inhibitory synapses in D2 medium spiny projection neurons (MSNs). (A) Schematic diagram showing differences in mIPSC amplitude according to location of the inhibitory synapses relative to the somatic recording electrode. **(B)** Reanalysis of mIPSC frequency in D2-MSNs from Figure 3, separating event by sex and amplitude: small (<10 pA) or large (>10 pA). **(C)** Examples of confocal images showing D2-eGFP fluorescence (upper left) used to create a somatic mask (upper middle) for analysis of perisomatic gephyrin-immunoreactive puncta (upper right). Lower row shows representative images for each genotype, with white dots highlighting gephyrin puncta. Scale bars: 2 um. **(D)** Cumulate probability plot of gephyrin puncta density for D2-MSNs from Oprm1+/+ (n=250 cells), Oprm1+/- (n=189 cells), and Oprm1-/- (n=223 cells) **(E)** Mean gephyrin puncta density for D2-MSNs from Oprm1+/+ (n=6 mice), Oprm1+/- (n=5 mice), and Oprm1-/- (n=6 mice). All groups contained similar numbers of female mice (open symbols) and male mice (closed symbols). Red asterisk indicates a significant Genotype x Amplitude interaction **(B)**; *p<0.05 comparing Oprm1 mutant to control with LSD post-hoc test **(B)** or Kolmogorov-Smirnov test **(D)**, or LSD post-hoc test between groups **(E)**.
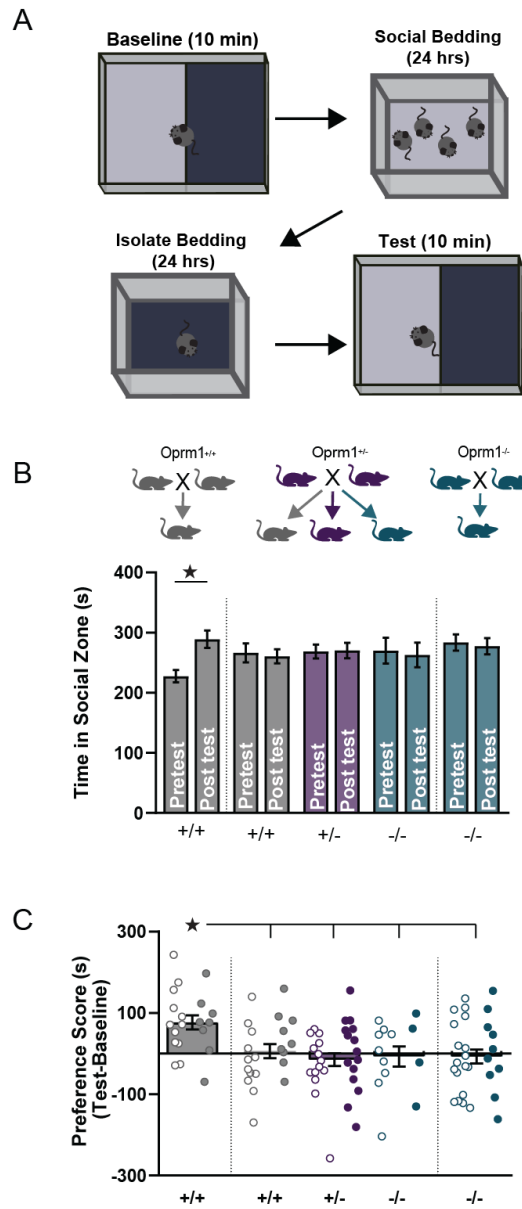
791 **Figure 5. Social conditioned place preference (CPP) as a function of Oprm1 genotype and breeding**
792 **strategy. (A)** Schematic diagram of the social CPP protocol. **(B)** Time spent in the social zone for mice of each
793 genotype generated by each breeding strategy (n=20/22/29/13/28, left to right), during the baseline session
794 before conditioning and the test session after conditioning. **(C)** Preference scores for the same groups of mice,
795 calculated as time in social zone on test minus baseline. All groups contained similar numbers of female mice
796 (open symbols) and male mice (closed symbols). *p<0.05 according to paired t-test **(B)** or LSD post-hoc test
797 **(C).**
798
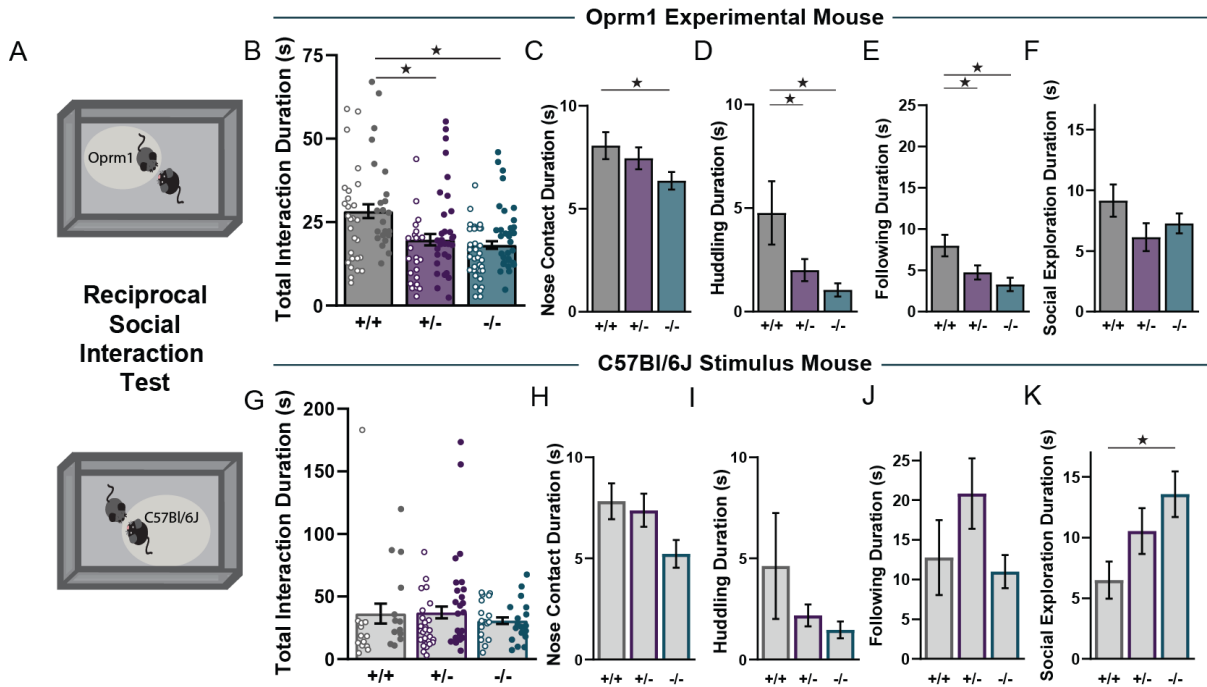
Figure 6. Oprm1 copy number influences on reciprocal social interaction. (A) Schematic diagram of the reciprocal social interaction test, separately highlighting behavior of the Orpm1 experimental mouse (top) and the C57Bl/6J stimulus mouse (bottom). **(B)** Total interaction durations for Oprm1+/+ (n=51), Oprm1+/- (n=54), and Oprm1-/- (n=67). **(C-F)** Duration of nose contact (C), huddling (D), following (E), and social exploration (F) for Oprm1+/+ (n=35), Oprm1+/- (n=45), and Oprm1 -/- (n=55) **(F)**. **(G)** Total interaction durations for C57Bl/6J stimulus mice interacting with Oprm1+/+ (n=26), Oprm1+/- (n=50), and Oprm1-/- (n=35). **(H-K)** Duration of nose contact (H), huddling (I), following (J), and social exploration (K) for C57Bl/6J stimulus mice interacting with Oprm1+/+ (n=20), Oprm1+/- (n=41), and Oprm1-/- (n=28). All groups contained similar numbers of female mice (open symbols) and male mice (closed symbols); *p<0.05 between groups, LSD post-hoc test.
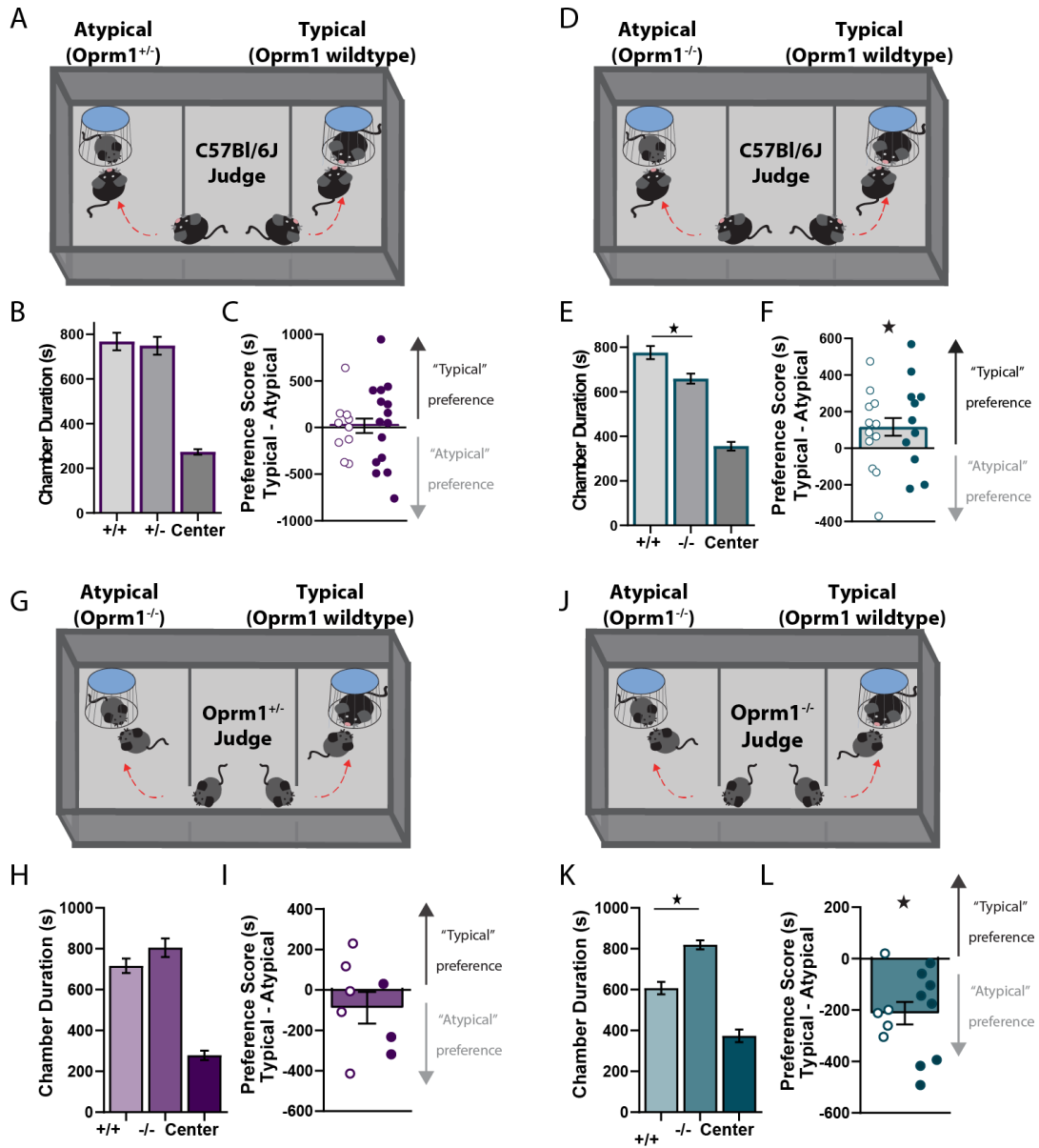
Figure 7. Real time social preference of C57Bl/6J and Oprm1 mutant judges. (A-C) C57Bl/6J judges (n=25) simultaneously engaging with social targets that are typical (Oprm1+/+) or atypical (Oprm1+/-), as shown in a schematic diagram (A), along with time spent in each chamber (B) and preference score (C). **(D-F)** C57Bl/6J judges (n=23) simultaneously engaging with social targets that are typical (Oprm1+/+) or atypical (Oprm1-/-), as shown in a schematic diagram (D), along with time spent in each chamber (E) and preference score (F). **(G-I)** Oprm1+/- judges (n=8) simultaneously engaging with social targets that are typical (Oprm1+/+) or atypical (Oprm1-/-), as shown in a schematic diagram (G), along with time spent in each chamber (H) and preference score (I). **(J-L)** Oprm1-/- judges (n=13) simultaneously engaging with social targets that are typical (Oprm1+/+) or atypical (Oprm1-/-), as shown in a schematic diagram (J), along with time spent in each

33

823   chamber (K) and preference score (L). All groups contained similar numbers of female mice (open symbols)
824   and male mice (closed symbols); *p<0.05 according to LSD post-hoc test **(E, K)** or one-sample t-test **(F, L)**.

825 **TABLES AND TABLE LEGEND**
826
827
828 **Table 1. List of primer sequences for quantitative RT-PCR**.
829

Gene Name	Symbol	Forward Oligonucleotide	Reverse Oligonucleotide
Beta-actin	Actb	GACGGCCAGGTCATCACAT	CCACCGATCCACACAGAGTA
Mu Opioid Receptor	Oprm1	TCTGCCCGTAATGTTCATGG	AGGCGAAGATGAAGACACAG
Gephyrin	Gphn	GACAGAGCAGTACGTGGAACTTCA	GTCACCATCATAGCCGTCCAA
VGAT	Slc32a1	CTATTCCACATCGCCCTGAT	AATTTGGTGGTGGTGGTGAT
Collybistin	Arhgef9	CCACCTCAGCGAGATAGGAC	GAGCTCCATGCAGGCATCCA
SAP97	Dlg1	CGTAGCTGCGCTGAACTAGA	AGAGCAAAGGGAAGCCAAAT
SAP102	Dlg3	AAGGCAGCAGCTTTCTCTTG	AATCAACACTTCCCGCTCAC
PSD95	Dlg4	AAGCTGGAGCAGGAGTTCAC	GAGGTCTTCGATGACACGTT

830
831

832
833 **Table 2. Social approach and memory of Oprm1 mutant mice in a standard three-chamber test.**
834

Genotype	Oprm1+/+ (47)	Oprm1+/- (52)	Oprm1-/- (53)
Social approach: time in chamber with C57Bl/6J stimulus mouse	292.3 ± 7.3	290.2 ± 7.0	296.8 ± 7.9
Social approach: time in chamber with empty cup	228.0 ± 6.4	229.2 ± 7.0	228.2 ± 7.4
Social approach: time in center chamber	78.2 ± 3.4	80.6 ± 3.0	75.0 ± 4.1
Social approach: statistical results	Chamber: $F_{1,146}=67.25$, $p<0.001$, $\eta_p^2=0.31$ Chamber x Genotype: $F_{12146}<1$		
Social memory: time in chamber with novel C57Bl/6J stimulus mouse	217.6 ± 6.8	223.8 ± 7.9	239.1 ± 8.1
Social memory: time in chamber with familiar C57Bl/6J stimulus mouse	281.6 ± 6.7	263.0 ± 8.4	257.4 ± 8
Social memory: time in center chamber	100.8 ± 4.4	103.1 ± 4.2	100.2 ± 5.6
Social memory: statistical results	Chamber: $F_{1,146}=18.19$, $p<0.001$, $\eta_p^2=0.11$ Chamber x Genotype: $F_{2,146}=2.47$, $p=0.088$		

835
836 All data are presented as mean +/- SEM; number in parenthesis represent sample sizes for each genotype.

36